Mass Spectrometry
DOI: 10.5702/massspectrometry.A0053

Original Article

Secondary Ion Mass Spectrometry Analysis of Renal Cell Carcinoma with Electrospray Droplet Ion Beams

Satoshi Ninomiya*[,1], Kentaro Yoshimura[2], Lee Chuin Chen[1], Sen Takeda[2], and Kenzo Hiraoka*[,3]

[1] *Interdisciplinary Graduate School, University of Yamanashi, 4–3–11 Takeda, Kofu, Yamanashi 400–8511, Japan*
[2] *Department of Anatomy and Cell Biology, Faculty of Medicine, University of Yamanashi, 1110 Shimokato, Chuo-shi, Yamanashi 409–3898, Japan*
[3] *Clean Energy Research Center, University of Yamanashi, 4–3–11 Takeda, Kofu, Yamanashi 400–8511, Japan*

Tissue samples from renal cell carcinoma patients were analyzed by electrospray droplet ion beam-induced secondary ion mass spectrometry (EDI/SIMS). Positively- and negatively-charged secondary ions were measured for the cancerous and noncancerous regions of the tissue samples. Although specific cancerous species could not be found in both the positive and negative secondary ion spectra, the spectra of the cancerous and noncancerous tissues presented different trends. For instance, in the *m*/*z* range of 500–800 of the positive secondary ion spectra for the cancerous tissues, the intensities for several *m*/*z* values were lower than those of the *m*/*z*+2 peaks (indicating one double bond loss for the species), whereas, for the noncancerous tissues, the inverse trend was obtained. The tandem mass spectrometry (MS/MS) was also performed on the tissue samples using probe electrospray ionization (PESI), and some molecular ions produced by PESI were found to be fragmented into the ions observed in EDI/SIMS analysis. When the positive secondary ion spectra produced by EDI/SIMS were analyzed by principal component analysis, the results for cancerous and noncancerous tissues were separated. The EDI/SIMS method can be applied to distinguish between a cancerous and a noncancerous area with high probability.

Please cite this article as: Mass Spectrom (Tokyo) 2017; 6(1): A0053

Keywords: SIMS, electrospray droplet, renal cell carcinoma

(Received October 19, 2016; Accepted December 10, 2016)

INTRODUCTION

Organic and biomolecular samples have been frequently analyzed by mass spectrometry with various ionization methods such as matrix-assisted laser desorption/ionization (MALDI) and electrospray ionization (ESI).[1–4] MALDI is an ionization method based on the ablation of analyte upon laser irradiation of a sample containing analyte incorporated into a matrix, and was first reported by Karas *et al.*[1] Tanaka *et al.* opened the road to the ionization of very large molecules.[2] ESI is based on the production of highly charged solvent droplets containing dissolved analyte, and was first reported by Fenn *et al.*[3,4] As these ionization techniques can ionize relatively large biomolecules with less fragmentation, they have been widely used for numerous applications in biotechnology.

Secondary ion mass spectrometry (SIMS), on the other hand, has been originally applied to the surface and interface analysis of inorganic materials such as metals and semiconductors.[5] The analytical method called static SIMS or time-of-flight SIMS (TOF-SIMS) was developed for organic materials by Benninghoven.[6] TOF-SIMS has been recently applied to the analysis of biological samples such as cells and tissues,[7,8] because cluster ion beams such as C_{60}^+ and Bi_3^+ can be used in SIMS instruments and the cluster beams can ionize biomolecules with higher efficiency than conventional atomic ion beams such as Ar^+ and Cs^+.[9,10] However, the ion formation efficiency for biomolecules under small cluster ion bombardment is still low and the available mass range for SIMS analysis is limited.

To improve the analytical performance of SIMS for

* Correspondence to: Satoshi Ninomiya, *Interdisciplinary Graduate School, University of Yamanashi, 4–3–11 Takeda, Kofu, Yamanashi 400–8511, Japan*, e-mail: sninomiya@yamanashi.ac.jp
* Correspondence to: Kenzo Hiraoka, *Clean Energy Research Center, University of Yamanashi, 4–3–11 Takeda, Kofu, Yamanashi 400–8511, Japan*, e-mail: hiraoka@yamanashi.ac.jp

biological samples, the effects of massive cluster ion beams have been studied. Mahoney *et al.* suggested massive cluster impact (MCI) as a new desorption and ionization method for relatively high-mass molecules such as proteins.[11,12] Williams *et al.* achieved SIMS imaging of biomolecular pattern samples using the MCI method coupled with a TOF secondary ion microscope instrument.[13] A lateral image resolution of ~3 μm was obtained for a bradykinin ion image. The gas cluster ion beam (GCIB), a technique originally developed for surface modification by Yamada *et al.*[14] is very successful for soft etching of organic materials. The depth profiling of organic materials with SIMS and X-ray photoelectron spectroscopy (XPS) is significantly improved by using Ar-GCIB as the etching beam.[15,16] In addition, the ionization efficiency when using H_2O vapor as the source gas of a GCIB has been studied, and water cluster ions such as $(H_2O)^+_{1000}$ have enhanced the secondary ion yields by a factor of 10 or more over Ar-GCIB for some biomolecular samples.[17,18]

The electrospray droplet ion (EDI) beam was suggested by Hiraoka *et al.*[19] as a new massive cluster ion beam, in which the charged water droplets are produced from an atmospheric-pressure electrospray of 0.01 M trifluoroacetic acid (TFA) aqueous solution. The EDI beams have achieved efficient ionization of relatively high-mass molecules,[19,20] low-damage etching of polymers,[21,22] and etching of metal oxides without reduction.[23,24] However, the SIMS performance of the EDI beams has not been sufficiently investigated for real-world biological samples. This paper reports on SIMS analysis induced by EDI beams of biological tissue samples from renal cell carcinoma patients and proposes to use the EDI/SIMS method as a tool for the identification of cancerous and noncancerous areas of the tissue samples with high probability.

EXPERIMENTAL

EDI/SIMS

Details of the EDI/SIMS procedure were described in our previous papers.[19,20] Briefly, charged water droplets were formed by an atmospheric-pressure electrospray of 10^{-2} M TFA aqueous solution, and were introduced into the vacuum system through a 400-μm-diameter orifice. The charged water droplet beams were roughly size-selected (m/z: 1×10^4–5×10^4) and transported by a first quadrupole ion guide, and then finally accelerated up to 10 kV after exiting the ion guide. The beam current and diameter on the target were typically 0.3–0.6 nA and 3 mm, respectively. The charged water droplet beams impacted the sample tissue held on a stainless steel holder, and the secondary ions produced from the tissue sample were transported into a second quadrupole ion guide and were mass-analyzed by an orthogonal time-of-flight mass spectrometer (TOF-MS, AccuTOF, JEOL, Tokyo, Japan). The base and working pressure in the sample chamber were 1×10^{-4} and 6×10^{-4} Pa, respectively, and both were 1.3×10^{-5} Pa in the mass spectrometer.

MS/MS analysis with probe electrospray ionization (PESI)

The collision-induced dissociation (CID) tandem mass spectrometry (MS/MS) measurements for the renal cell carcinoma (RCC) tissue samples were performed using an ion trap mass spectrometer (LTQ-XL, Thermo Fisher Scientific, San Jose, CA, USA). The PESI method was adopted to pick up the tissue sample and ionize it. PESI is one of the atmospheric-pressure ionization methods developed by Hiraoka *et al.*,[25] and was used for ambient mass spectrometry. Details of the PESI procedure were described elsewhere.[25,26] Briefly, a disposable acupuncture needle (J type No. 02, SEIRIN, Shizuoka, Japan) was moved up and down in a direction normal to the axis of the sampling capillary on the mass spectrometer with a linear actuator system (SCN5-010-050-S03, Dyadic Systems, Kanazawa, Japan). The lowest position of the actuator system was adjusted so that the needle tip touched the tissue sample and picked-up a few pL of its fluid.[27] At the highest position, 2.0 kV was applied to the needle and the fluid sample loaded on the tip was electrosprayed in atmospheric pressure.

Samples

All the examined kidney tissue samples from RCC patients were provided from the University of Yamanashi Hospital. Tissue samples were divided into noncancerous and cancerous regions, and were immediately frozen for storage. These tissue samples were analyzed by EDI/SIMS and PESI/MS/MS without any pretreatment. Informed consent was obtained from all the patients before resection. All the procedures concerning human materials and experiments were reviewed and approved by the ethical committee of the University of Yamanashi.

The pure glyceryl trioleate ($C_{57}H_{104}O_6$, molecular weight: 885.43) sample was purchased from Merck (Darmstadt, Germany), and used for EDI/SIMS analysis without further purification. 180 mg of the sample was dissolved in an appropriate 1 mL solvent (chloroform : ethanol : water=60 : 30 : 4.5) and a 10-μL aliquot of the sample solution was deposited on the stainless steel holder with a 3 mm spot size diameter. The sample was dried at room temperature and then introduced into the vacuum chamber.

RESULTS AND DISCUSSION

EDI/SIMS and MS/MS analysis for the tissue samples

Positively- and negatively-charged secondary ions were analyzed for the cancerous and noncancerous tissue samples from the RCC patients using the EDI/SIMS method. Examples of positive and negative secondary ion spectra of cancerous and noncancerous tissue samples are presented in Fig. 1. The insets for the positive ion spectra (Figs. 1(a) and (b)) also include photographs of the two types of the target holders with the respective types of cancerous and noncancerous tissue samples. As shown in Fig. 1, a wide variety of the positive and negative secondary ions was detected for the two types of tissue samples, and it is extremely difficult to annotate all of the secondary ions. Therefore, we will confine our discussion to some well-known species in SIMS. In the positive secondary ion spectra (Figs. 1(a) and (b)), the ion at m/z 184 was detected with the highest intensity for both the cancerous and noncancerous tissue samples. This ion is often observed in the SIMS spectra, and is known as phosphatidylcholine head group ($C_5H_{15}NPO_4^+$).[28,29] The ion at m/z 369 was detected with high intensity for the cancerous tissue sample (Fig. 1(a)), but had a relatively low inten-

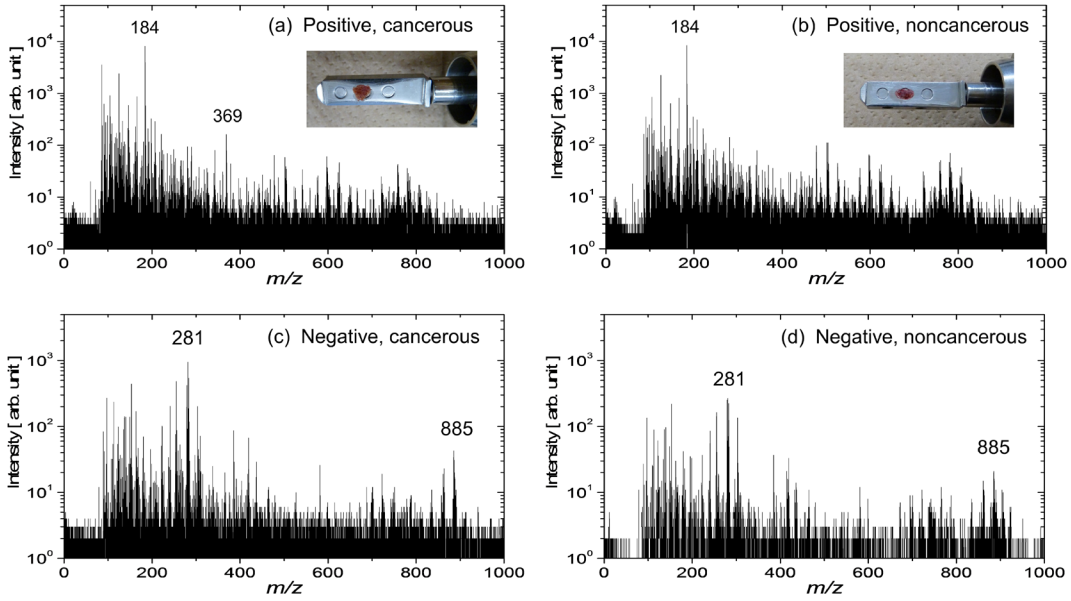

Fig. 1. Positive and negative secondary ion spectra for the cancerous and noncancerous tissue samples from a RCC patient. Each measurement was taken for 30 s with the orthogonal TOF-MS.

sity for the noncancerous tissue sample (Fig. 1(b)). This ion is also often observed in the SIMS spectra, and is annotated as protonated dehydrated cholesterol ($[(M-H_2O)+H]^+$).[30,31] In the negative secondary ion spectra, the characteristic ions at *m*/*z* 281 and *m*/*z* 885 were observed with high intensity for both the cancerous and noncancerous tissue samples, and were respectively assumed to be the typical negative secondary ions of fatty acid and phosphatidylinositol.[32,33] As a general tendency, in the negative secondary ion spectra, the signal intensities from the cancerous tissues were higher than from the noncancerous tissues, although we could not clearly confirm specific ions from either type.

The positive secondary ion spectra for cancerous and noncancerous tissue samples with *m*/*z* range between 400 and 900 are shown in Figs. 2(a) and (b), respectively. Many positive secondary ions were detected, and the signal intensities from the cancerous tissues were higher than from the noncancerous ones. The relative intensities of secondary ions with *m*/*z* values that were close to each other gave the characteristic trends as follows; for the cancerous tissues, the relative intensities of the secondary ions were often *m*/*z* 502>504, 597>599 and 780>782, whereas, the relative intensities for the noncancerous tissues were *m*/*z* 502<504, 597<599 and 780<782. However, the results described above were not always obtained for all the RCC patients, and some fluctuations were observed.

The tissue samples from the RCC patients used in this study were also analyzed using PESI mass spectrometry (PESI-MS) in a separate study by Yoshimura *et al.*[34] In the PESI method, the acupuncture needle was used as a sampling probe as well as electrospray emitter. The frozen tissue samples were quickly thawed at room temperature, and were then, directly analyzed without any pretreatment. Ions originating from phosphatidylcholines (PCs) (*e.g.*, PC[34:1], PC[34:2], PC[36:2], *m*/*z* range: 750–830) were shared by both the cancerous and noncancerous regions, possibly because they are the principal components of cell membranes. In addition, some triacylglycerol (TAG) peaks (*e.g.*, TAG[52:2], TAG[54:2], TAG[54:3], *m*/*z* range: 860–930)

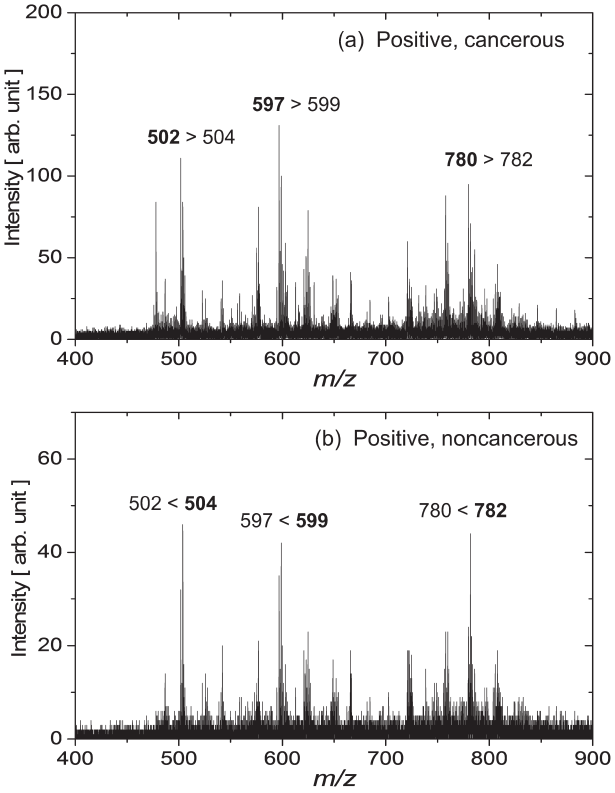

Fig. 2. Positive secondary ion spectra for the cancerous and noncancerous RCC tissue samples. Each measurement was taken for 120 s.

were detected with high intensity only for the cancerous tissues in PESI-MS positive ion spectra. In the EDI/SIMS positive ion spectra, the ions between the *m*/*z* 750 and 830 were also detected for both the cancerous and noncancerous tissues (Fig. 2), and these ions (typically at *m*/*z* 780 and 782) were assumed to be from the PCs. However, the ions in the range between *m*/*z* 860 and 930 were rarely detected, even in the EDI/SIMS positive ion spectra for the cancerous tissue

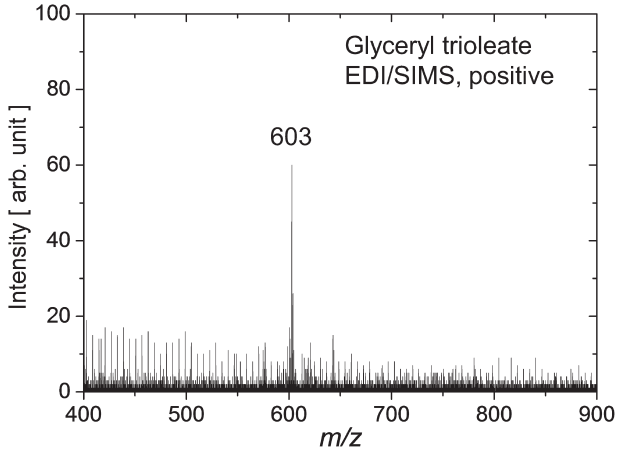

Fig. 3. Positive secondary ion spectrum of a pure TAG sample produced by EDI/SIMS.

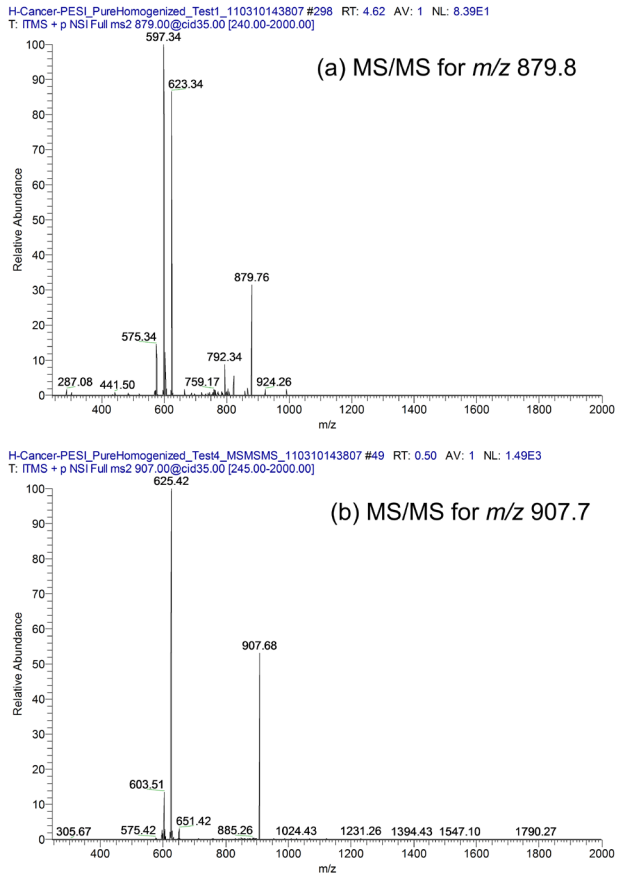

Fig. 4. MS/MS spectra for the species with *m*/*z* 879.8 (a) and 907.7 (b) obtained by PESI-MS from the cancerous tissue samples.

sample (Figs. 1 and 2). On the other hand, in the EDI/SIMS positive ion spectra, the ions between *m*/*z* 500 and 700 were detected with high intensity, but there were only a few peaks in this *m*/*z* range in the PESI-MS positive ion spectra.[34]

Next, we will consider the origin of the positive ions between *m*/*z* 500 and 700 that are observed frequently in the EDI/SIMS analysis. As the TAG ions were detected with high intensity for the same tissue sample using the PESI-MS method, secondary ions originating from TAGs should be produced by the EDI/SIMS method. Moreover, TAGs are well-known to be one of the main components of RCC.[34] First, we checked the positive secondary ion spectrum of a typical TAG sample using EDI/SIMS. The EDI/SIMS spectrum of a pure glyceryl trioleate (TAG[54:3], 18:1/18:1/18:1) sample is shown in Fig. 3. As clearly shown in the figure, the TAG molecular ions were rarely observed, and instead, the ion at *m*/*z* 603 was detected as a form of diacylglycerol (DAG) molecule. It was also reported that the signal intensity of the TAG molecule was extremely low and the ion at *m*/*z* 603 was clearly observed when the pure TAG sample was analyzed by SIMS with Bi cluster probes.[35] Therefore, the DAG ions originated from TAG molecules are considered to be mainly formed in SIMS measurements.

In addition, a CID-MS/MS (CID voltage: 35 V) analysis for the RCC tissue samples was performed using the ion trap mass spectrometer to confirm whether the TAG ions produced by PESI-MS for the actual tissue samples were fragmented into the ions observed in EDI/SIMS analysis. The MS/MS spectra for the precursors of *m*/*z* 879.8 and 907.7 obtained by PESI-MS from the cancerous tissue sample are shown in Fig. 4. The ion at *m*/*z* 879.8 was dissociated into the ions at *m*/*z* 575, 597, and 623, whereas *m*/*z* 907.7 was dissociated into the ions at *m*/*z* 603, 625, and 651. In fact, all the ions that dissociated from *m*/*z* 879.8 and 907.7 were observed in the EDI/SIMS spectra of the tissue samples. From these results, some of the secondary ions observed in the *m*/*z* range between 500 and 700 were assumed to have originated from TAGs. However, it is extremely difficult to annotate most of the secondary ions observed for the tissue samples in EDI/SIMS spectra. For the RCC tissue samples, more peaks were produced by EDI/SIMS than by PESI-MS. The amount of information obtained by EDI/SIMS is believed to be very rich, but further research is required to extract useful information from these spectra. For EDI/SIMS, the tissue sample must be placed in a high vacuum, and this analysis requires more effort and time than PESI-MS.

Principal component analysis (PCA) for the EDI/SIMS spectra

Finally, we examined the applicability of EDI/SIMS method for possible identification of cancerous or noncancerous tissue. As described in the former section, the relative intensities of positive secondary ions with *m*/*z* values that were close to each other gave the characteristic trends such as 780>782 for the cancerous tissues. However, the trends were not always obtained for all the tissue samples, and it is very difficult to determine whether a tissue sample is cancerous or not by observing the signal intensities of some specific ions in a spectrum. In order to interpret complex spectra data with higher accuracy, it becomes important to grasp the features of the whole spectrum by statistical analysis. Recently, multivariate analysis (MVA) methods have become standard tools for simplifying the interpretation of mass spectra.[36,37] MVA can significantly simplify a dataset by providing a comprehensive description of the data using a small number of variables. Among them, PCA is one of the most widely employed MVAs for the analysis of mass spectra, and the PCA is known as a method to elucidate relationships between variables in the mass spectra.[37] In PCA, a dataset composed of multiple mass spectra is evaluated using three parameters, called “factor,” “loadings” and “scores.”

PCA was applied to the spectra dataset obtained from

seven cancerous and seven noncancerous tissue samples from five RCC patients from the University of Yamanashi Hospital. Before PCA was applied to this dataset, each spectrum was preprocessed with the normalization method, so that the total intensity of the *m/z* signals was 1. Figure 5(a) shows the 2D scores of first and second PCA factors (PC1 and PC2, respectively). PC1 indicates the direction of the largest variance of data points in the dataset and has the largest associated eigenvalue, and PC2 is the direction orthogonal to PC1 that captures the largest spread not accounted by PC1.[37] The scores indicate the projection of the samples onto a factor, reflecting the relationship between the samples. As shown in Fig. 5(a), each spectrum from the cancerous and noncancerous tissue samples was clearly separated by the scores. In this case, because PC2 distinguishes between cancerous and noncancerous tissues, we could classify spectra with positive PC2 scores as cancerous and spectra with negative PC2 scores as noncancerous. Figure 5(b) shows the 2D loadings of PC1 and PC2 for several *m/z* species. The loadings indicate correlation between the original variables and a factor, reflecting the covariance relationship between variables.[37] Also in this case, we could classify ion species with positive PC2 loadings as special for cancerous tissue and ion species with negative PC2 loadings as special for noncancerous tissue. That is, the ions at *m/z* 502, 597, and 780 could be summarized as special for the cancerous tissue, whereas those at *m/z* 504, 599, and 782 could be summarized as special for noncancerous. These assumptions are in good agreement with the results shown in Fig. 2. From the results for the kidney tissue samples, the EDI/SIMS method could be applied to identify a cancerous from a noncancerous area with high probability. Moreover, the EDI/SIMS method might be applied to support diagnostic studies for various biological samples.

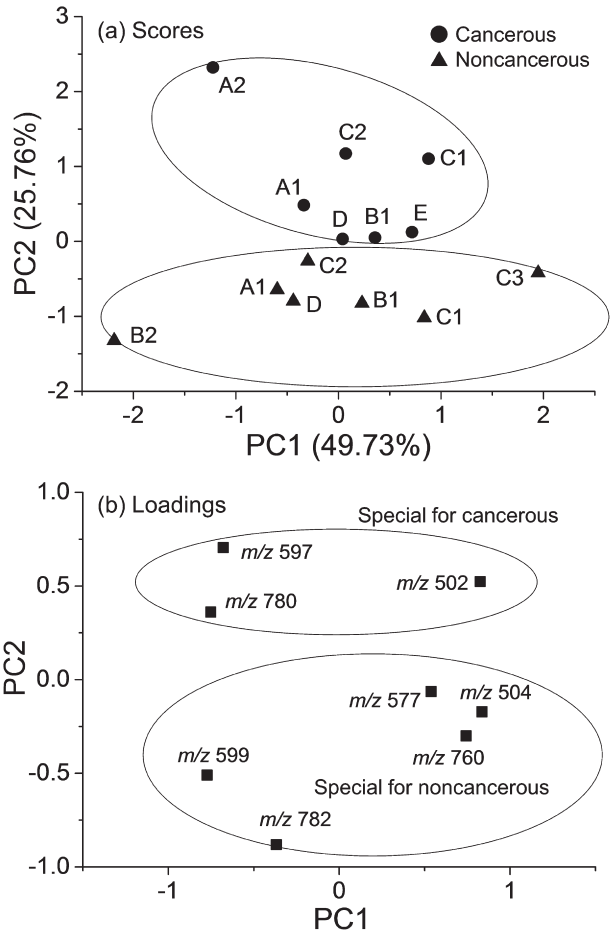

Fig. 5. Scores (a) and loadings (b) of PC1 and PC2 for the 14 tissue samples measured with EDI/SIMS method. The circles shown are visual guides only.

CONCLUSION

EDI/SIMS analysis was applied to the cancerous and noncancerous tissue samples from RCC patients, and positively- and negatively-charged secondary ions were mass-analyzed by an orthogonal TOF-MS. Various positive and negative secondary ions were detected for both the cancerous and noncancerous tissue samples, and the spectra obtained for the cancerous and noncancerous tissues indicated different trends in relative intensities of secondary ions with *m/z* values that were close to each other. When comparing the positive ion spectra measured with the EDI/SIMS and PESI-MS methods, ions originating from PCs (*m/z* 750–830) were observed for both methods, but the strong TAG signals observed by PESI-MS were not detected by EDI/SIMS. It is assumed that in the EDI/SIMS analysis TAGs were fragmented into DAGs and detected in the *m/z* range between 500 and 700. As the dataset of seven cancerous and seven noncancerous spectra obtained with EDI/SIMS was analyzed by PCA, the different spectra from the cancerous and noncancerous tissue samples were clearly separated. From these results, the EDI/SIMS method could identify the cancerous or noncancerous areas for the tissue samples with high probability. In addition, this method might be applied to support diagnostic studies for various biological samples.

Acknowledgements

We would like to thank Dr. T. Miyamoto and Prof. M. Takeda of the Department of Urology, Faculty of Medicine, University of Yamanashi for the supply of the RCC tissue samples. This work was partly supported by the Grant-in-Aid for Scientific Research (C) from Japan Society for the Promotion of Science (JSPS) of the Japanese government (JSPS KAKENHI Grant No. 26505004).

REFERENCES

1) M. Karas, D. Bachmann, U. Bahr, F. Hillenkamp. Matrix-assisted ultraviolet laser desorption of non-volatile compounds. *Int. J. Mass Spectrom. Ion Process.* 78: 53–68, 1987.
2) K. Tanaka, H. Waki, Y. Ido, S. Akita, Y. Yoshida, T. Yoshida, T. Matsuo. Protein and polymer analyses up to *m/z* 100000 by laser ionization time-of flight mass spectrometry. *Rapid Commun. Mass Spectrom.* 2: 151–153, 1988.
3) M. Yamashita, J. B. Fenn. Electrospray ion source. Another variation on the free-jet theme. *J. Phys. Chem.* 88: 4451–4459, 1984.
4) J. B. Fenn, M. Mann, C. K. Meng, S. F. Wong, C. M. Whitehouse. Electrospray ionization for mass spectrometry of large biomolecules. *Science* 246: 64–71, 1989.
5) D. Briggs, M. P. Seah (Eds). Practical Surface Analysis 2nd Ed. Vol. 2 Ion and Neutral Spectroscopy, John Wiley & Sons Ltd., Sussex, U.K., 1992.
6) A. Benninghoven. Analysis of submonolayers on silver by nega-

tive secondary ion emission. *Phys. Status Solidi* 34: K169–K171, 1969.
7) D. Touboul, F. Halgand, A. Brunelle, R. Kersting, E. Tallarek, B. Hagenhoff, O. Laprévote. Tissue molecular ion imaging by gold cluster ion bombardment. *Anal. Chem.* 76: 1550–1559, 2004.
8) N. Winograd. The magic of cluster SIMS. *Anal. Chem.* 77: 142A–149A, 2005.
9) D. Weibel, S. Wong, N. Lockyer, P. Blenkinsopp, R. Hill, J. C. Vickerman. A C_{60} primary ion beam system for time of flight secondary ion mass spectrometry: Its development and secondary ion yield characteristics. *Anal. Chem.* 75: 1754–1764, 2003.
10) F. Kollmer. Cluster primary ion bombardment of organic materials. *Appl. Surf. Sci.* 231–232: 153–158, 2004.
11) J. F. Mahoney, J. Perel, S. A. Ruatta, P. A. Martino, S. Husain, T. D. Lee. Massive cluster impact mass spectrometry: A new desorption method for the analysis of large biomolecules. *Rapid Commun. Mass Spectrom.* 5: 441–445, 1991.
12) J. F. Mahoney, D. S. Cornett, T. D. Lee. Formation of multiply charged ions from large molecules using massive-cluster impact. *Rapid Commun. Mass Spectrom.* 8: 403–406, 1994.
13) J. Zhang, K. Franzreb, P. Williams. Imaging with biomolecular ions generated by massive cluster impact in a time-of-flight secondary ion microscope. *Rapid Commun. Mass Spectrom.* 28: 2211–2216, 2014.
14) I. Yamada, J. Matsuo, N. Toyoda, A. Kirkpatrick. Materials processing by gas cluster ion beams. *Mater. Sci. Eng. R* 34: 231–295, 2001.
15) S. Ninomiya, K. Ichiki, H. Yamada, Y. Nakata, T. Seki, T. Aoki, J. Matsuo. Precise and fast secondary ion mass spectrometry depth profiling of polymer materials with large Ar cluster ion beams. *Rapid Commun. Mass Spectrom.* 23: 1601–1606, 2009.
16) T. Miyayama, N. Sanada, M. Suzuki, J. S. Hammond, S.-Q. D. Si, A. Takahara. X-ray photoelectron spectroscopy study of polyimide thin films with Ar cluster ion depth profiling. *J. Vac. Sci. Technol. A* 28: L1–L4, 2010.
17) S. Sheraz née Rabbani, A. Barber, J. S. Fletcher, N. P. Lockyer, J. C. Vickerman. Enhancing secondary ion yields in time of flight-secondary ion mass spectrometry using water cluster primary beams. *Anal. Chem.* 85: 5654–5658, 2013.
18) S. Sheraz née Rabbani, I. B. Razo, T. Kohn, N. P. Lockyer, J. C. Vickerman. Enhancing ion yields in time-of-flight-secondary ion mass spectrometry: A comparative study of argon and water cluster primary beams. *Anal. Chem.* 87: 2367–2374, 2015.
19) K. Hiraoka, D. Asakawa, S. Fujimaki, A. Takamizawa, K. Mori. Electrosprayed droplet impact/secondary ion mass spectrometry. *Eur. Phys. J. D* 38: 225–229, 2006.
20) K. Hiraoka, K. Mori, D. Asakawa. Fundamental aspects of electrospray droplet impact/SIMS. *J. Mass Spectrom.* 41: 894–902, 2006.
21) K. Hiraoka, Y. Sakai, Y. Iijima. Surface analysis of polyimide bombarded by charged water droplets. *J. Vac. Sci. Technol. A* 28: 510–514, 2010.
22) Y. Sakai, Y. Iijima, D. Asakawa, K. Hiraoka. XPS depth profiling of polystyrene etched by electrospray droplet impact. *Surf. Interface Anal.* 42: 658–661, 2010.
23) Y. Sakai, S. Ninomiya, K. Hiraoka. X-ray photoelectron spectroscopy depth analysis of metal oxides by electrospray droplet impact. *Surf. Interface Anal.* 43: 1605–1609, 2011.
24) Y. Sakai, S. Ninomiya, K. Hiraoka. XPS depth analysis of CuO by electrospray droplet impact. *Surf. Interface Anal.* 44: 938–941, 2012.
25) K. Hiraoka, K. Nishidate, K. Mori, D. Asakawa, S. Suzuki. Development of probe electrospray using a solid needle. *Rapid Commun. Mass Spectrom.* 21: 3139–3144, 2007.
26) L. C. Chen, K. Nishidate, Y. Saito, K. Mori, D. Asakawa, S. Takeda, T. Kubota, H. Hori, K. Hiraoka. Characteristics of probe electrospray generated from a solid needle. *J. Phys. Chem. B* 112: 11164–11170, 2008.
27) K. Yoshimura, L. C. Chen, D. Asakawa, K. Hiraoka, S. Takeda. Physical properties of the probe electrospray ionization (PESI) needle applied to the biological samples. *J. Mass Spectrom.* 44: 978–985, 2009.
28) N. Bourdos, F. Kollmer, A. Benninghoven, M. Ross, M. Sieber, H.-J. Galla. Analysis of lung surfactant model systems with time-of-flight secondary ion mass spectrometry. *Biophys. J.* 79: 357–369, 2000.
29) P. Sjövall, J. Lausmaa, B. Johansson. Mass spectrometric imaging of lipids in brain tissue. *Anal. Chem.* 76: 4271–4278, 2004.
30) L. A. McDonnell, S. R. Piersma, A. F. Maarten Altelaar, T. H. Mize, S. L. Luxembourg, P. D. E. M. Verhaert, J. van Minnen, R. M. A. Heeren. Subcellular imaging mass spectrometry of brain tissue. *J. Mass Spectrom.* 40: 160–168, 2005.
31) P. D. Piehowski, A. J. Carado, M. E. Kurczy, S. G. Ostrowski, M. L. Heien, N. Winograd, A. G. Ewing. MS/MS methodology to improve subcellular mapping of cholesterol using TOF-SIMS. *Anal. Chem.* 80: 8662–8667, 2008.
32) M. K. Passarelli, N. Winograd. Lipid imaging with time-of-flight secondary ion mass spectrometry (ToF-SIMS). *Biochim. Biophys. Acta* 1811: 976–990, 2011.
33) N. Tahallah, A. Brunelle, S. De La Porte, O. Laprévote. Lipid mapping in human dystrophic muscle by cluster-time-of-flight secondary ion mass spectrometry imaging. *J. Lipid Res.* 49: 438–454, 2008.
34) K. Yoshimura, L. C. Chen, M. K. Mandal, T. Nakazawa, Z. Yu, T. Uchiyama, H. Hori, K. Tanabe, T. Kubota, H. Fujii, R. Katoh, K. Hiraoka, S. Takeda. Analysis of renal cell carcinoma as a first step for developing mass spectrometry-based diagnostics. *J. Am. Soc. Mass Spectrom.* 23: 1741–1749, 2012.
35) P. Malmberg, H. Nygren, K. Pichter, Y. Chen, F. Dangardt, P. Friberg, Y. Magnusson. Imaging of lipids in human adipose tissue by cluster ion TOF-SIMS. *Microsc. Res. Tech.* 70: 828–835, 2007.
36) J. L. S. Lee, B. J. Tyler, M. S. Wagner, I. S. Gilmore, M. P. Seah. The development of standards and guides for multivariate analysis in surface chemical analysis. *Surf. Interface Anal.* 41: 76–78, 2009.
37) J. L. S. Lee, I. S. Gilmore, M. P. Seah. Quantification and methodology issues in multivariate analysis of ToF-SIMS data for mixed organic systems. *Surf. Interface Anal.* 40: 1–14, 2008.